LC-TH-2001-030

Hadronic Cross-sections in $\gamma\gamma$ Processes at the Next Linear Collider

Rohini M. Godbole
Centre for Theoretical Studies, Indian Institute of Science, Bangalore 560 012, India.
E-mail: rohini@cts.iisc.ernet.in

G. Pancheri
Laboratori Nazionali di Frascati dell'INFN, Via E. Fermi 40, I 00044, Frascati, Italy.
E-mail: Giulia.Pancheri@lnf.infn.it

A. De Roeck
CERN, 1211 Geneva 23, Switzerland.
E-mail: deroeck@mail.cern.ch

Abstract

In this note we address the measurability of the hadronic cross-sections for $\gamma\gamma$ processes at a high energy linear e^+e^- collider. We present an estimate of the accuracy with which this cross-section needs to be measured, in order to distinguish between the different theoretical models which try to 'explain ' the rise of total cross-sections with energy. We find that the precision of the measurement required to distinguish the EMM type models from the proton-like models, for $300 < \sqrt{s}_{\gamma\gamma} < 500$ GeV, is $\lesssim$20%, whereas to distinguish between various proton-like models or among the different parametrizations of the eikonalized minijet models, a precision of $\lesssim$8−9% or $\lesssim$6−7% respectively, is required.

1 Introduction

The rising total cross-section in proton-proton collisions was a very early indication of QCD processes at work, reflecting the fact that the increasing energy allows for deeper and deeper probe of the structure of the colliding particles[1] leading to liberation of more and more constituents, resulting in higher scattering probability. The proton-proton and proton-antiproton cross-sections are now known experimentally to a very good precision. We do not yet fully understand these cross-sections from first principles, but there are various models of hadronic interactions whose parameters can be completely fixed by the data and which then allow for good predictions of the total cross-section in the high energy region, certainly up to LHC energies. Thus, although not everything is calculable from first principles in QCD, there is no problem as far as predicting the total hadronic production at future accelerators is concerned.

The situation is substantially different for the photon induced processes. This renders the issue of measurement of the total $\gamma\gamma$ cross-section at energies in the region 300-500 GeV range very important both from the theoretical point of view, as well as experimental. Indeed, the question of hadron production in $\gamma\gamma$ collisions is interesting from a point of view of achieving a good theoretical understanding of the rise of the hadronic cross-sections with energy, in the framework of QCD or otherwise, as well as from a much more pragmatic viewpoint of being able to estimate the hadronic backgrounds at the next linear colliders [2]. There exist two classes of models which have been suggested in the context of rise of the hadronic cross-sections in pp and $\bar{p}p$ processes. All of these 'explain' the rise for the pp and $\bar{p}p$ case equally well but differ greatly in their predictions for $\gamma\gamma$ collisions even at the modest values of the $\gamma\gamma$ energies that are currently available. HERA and LEP have opened the way to an entire new field in QCD, the study of the hadronic interactions of the photon in terms of its quark and gluon content [3]. Hadronic collisions show the beginning of the rise to take place at centre of mass energies below 100 GeV but to determine the steepness of the rise one needs points in the 300-500 GeVand even higher. Thus, as in the case of hadron collisions, to gain a good theoretical understanding of the total cross-section for $\gamma\gamma$ processes, one needs much higher energies and better statistics than the one currently available from LEP and HERA.

At LEP phase space limits the c.m. energy of the $\gamma\gamma$ system to about

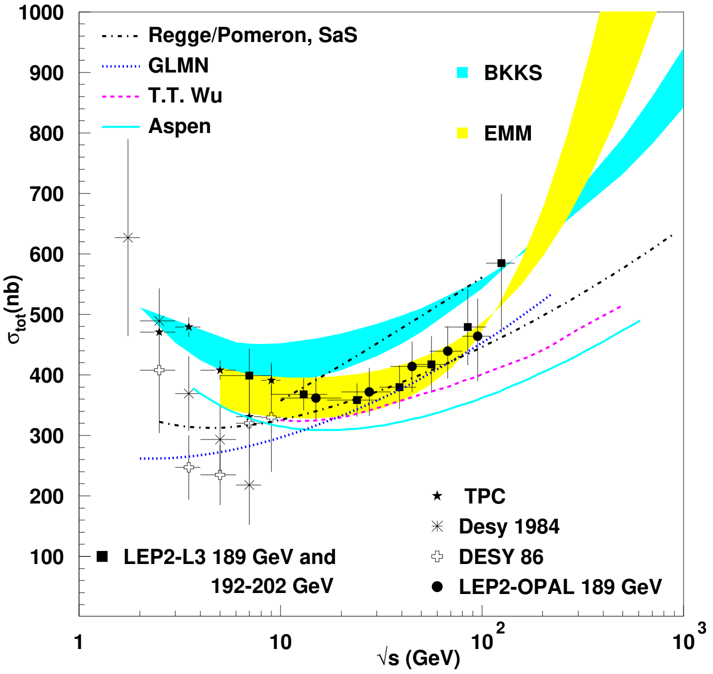

Figure 1: The predictions from from factorization models, Regge-Pomeron exchange and a QCD structure function models together with those from the EMM and a comparison with present data.

100 GeV, at HERA $\sqrt{s_{\gamma p}}$ is higher, but then the presence of proton partly obscures the issue. Note that, until five years ago, the available data for $\gamma\gamma$ processes did not yet show any rise, stopping short of $\sqrt{s} = 20$ GeV and with very large errors. L3 [4, 5] and OPAL [6] data have drastically changed the situation. Presently, the $\gamma\gamma$ cross-section data show a very clear rise, which may be even stronger than in hadron-hadron collisions [7] but there are a number of theoretical and experimental issues, which only the Linear Collider(LC) can clarify, by reaching higher energies and statistics.

A review of the theoretical ideas and issues was presented in [8]. In Fig.1 we have plotted the recent data from LEP and from lower energies with the predictions from "proton-like" models, labelled SaS[9], Aspen[10], BSW[11], as well as from QCD and Regge inspired models, like the curve labelled GLMN[12] and the band labelled BKKS[13]. The band labelled EMM corresponds to the two formulations, inelastic and total. For the EMM, we have used two sets of representative parameters, both of which are obtained from the γp cross-section following the procedure outlined in [14]. All models predict a rise of the cross-section with the collision energy $\sqrt{s}_{\gamma\gamma}$. The predictions for high energies show dramatic differences reflecting our present lack in understanding. In proton-like models (solid curve [10]), the rise follows closely that of the proton-proton cross-section, while in QCD based models (upper [13] and lower [8] bands), the rise is obtained using the eikonalized pQCD jet cross-section.

In this note we will examine closer the experimental issues involved in measuring two-photon interactions at a future high energy e^+e^-collider.

2 Linear Colliders

Two photon processes at future high energy linear colliders can be measured either as in a storage ring, via photon emission from the lepton beams, according to a Weizsäcker Williams(WW)[15] energy distribution, or using the LC in a photon collider mode [16]. In the latter case the high energy electron beam is converted into a high energy photon beam, by backscattering of photons of an intense laser beam, just before the interaction point. The maximum energy of the generated photons is given by $E_\gamma^{max} = xE_e/(1+x)$, with E_e the electron beam energy and $x = 4E_eE_L\cos^2(\theta/2)/m_e^2c^4$ with E_L and θ the laser photon energy and angle between the electron and laser beam. The distance of the conversion to the interaction point is in the range of several mm to a few cm. A typical value for x is 4.8, which leads to photon spectra which peak around $0.8E_e$. Hence, a typical distribution of $\gamma\gamma$ luminosity as a function of the invariant mass peaks at the maximum reachable invariant mass of around $0.8\sqrt{s}_{e^+e^-}$ with widths of $\approx 0.10-0.15$ for $\gamma\gamma$ collisions. The 'luminosity' is usually defined to be the luminosity corresponding to the region $0.64 < \sqrt{s_{\gamma\gamma}} < \sqrt{s_{\gamma\gamma,max}}$ and is typically 10% of the geometrical e^+e^- luminosity $\mathrm{L_{geom}}$. However, since the electron beams are converted before collision, smaller β functions at the interaction point can be allowed for. This can make up for part of the luminosity lost compared to an e^+e^- collider, by using smaller beam spots. For the TESLA [17] one finds $L_{\gamma\gamma} \simeq 0.35 L_{e^+e^-}$ This leads to event samples corresponding of order 100 fb^{-1} per year for the PLC.

In this study the PHOJET [18] program was used which has an option for the backscattered laser photon spectrum. Both the e$^+$e$^-$and BL modes of the LC will be investigated. Detector effects were studied with the program SIMDET [19].

3 Experimental study

First we consider the case for the e$^+$e$^-$collider mode. Present experiments at LEP which measure the two photon cross-section are hampered by experimental and detector limitations. For two photon events with on mass shell photons, the electrons disappear in the beam-pipe, so the only information available is the hadronic final state. Hence the variable $\sqrt{s}_{\gamma\gamma}$ needs to be reconstructed from the visible hadronic final state in the detector. At the highest energies the hadronic final state extends in pseudorapidity $\eta = \ln\tan\theta/2$ in the region $-8 < \eta < 8$, as shown in Fig. 2a, while a typical LC detector covers roughly the region $-3 < \eta < 3$. Hence the correlation of the measured $\sqrt{s}_{\gamma\gamma}$compared to the true one will be even poorer at the LC than at LEP, as shown in Fig. 2b. However, some information can be obtained by measuring the total integrated cross-section above a value $\sqrt{s}_{\gamma\gamma}$, see Section 5.

For a $\gamma\gamma$ collider the photon beam energy can be tuned with a spread of less than 10%, such that measurements of $\sigma^{tot}_{\gamma\gamma}$ can be made at a number of "fixed" energy values in e.g. the range $100 < \sqrt{s}_{\gamma\gamma} < 400$ GeV by changing the beam energy of the collider, as shown in Fig. 2c. For the spectra shown it was assumed in the simulation that the same value of x is kept at each energy, which means that the wavelength of the laser needs to be changed at each beam energy. A more likely scenario is that the same laser is used at the lower energies, which will then have correspondingly different x values, and thus somewhat different spectra.

Events were selected with $\sqrt{s_{\gamma\gamma}}(vis) > 10$ GeV, and a minimum of 3 charged tracks detected in the experiment. The acceptance for non-diffractive events is about 95%. Diffractive non-elastic events are accepted with 35% efficiency, while elastic events are essentially lost. Hence to measure the total cross-section with sufficient precision specially designed measurements for the diffractive components will be required. To that end also measurements at lower energy (e.g. LEP) will be useful, in order to extrapolate the elastic component. A technique to measure diffractive contributions separately, mirrored to the rapidity gap methods used at HERA, has been proposed in [20]. We will assume here that such measurements will be made, and reduce the systematic error due to the diffractive component.

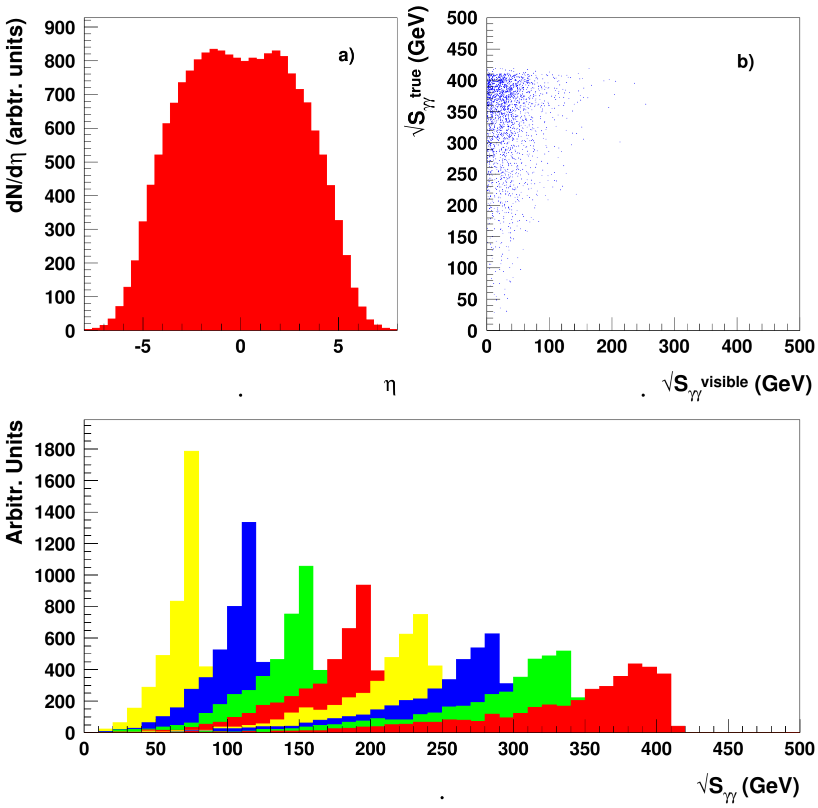

Figure 2: For $\gamma\gamma$ collisions at $\sqrt{s} = 400$ GeV: a) η distribution of produced particles; b) correlation between the true and visible $\sqrt{s}$; c) luminosity spectra for eight measurements of σ_{tot} at different energies.

The absolute precision with which these cross-sections can be measured ranges from 5% to 10%, where the largest contributions to the errors are due

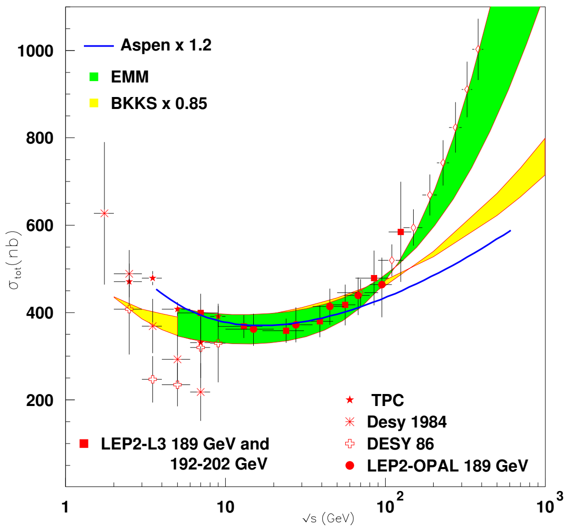

Figure 3: The total $\gamma\gamma$ cross-section as function of the collision energy, compared with model calculations: BKKS band (upper and lower limit correspond to different photon densities [13]); a proton-like model (solid line [10]); EMM band (Eikonal Minijet Model for total and inelastic cross-section, with different photon densities and different minimum jet transverse momentum [8]). The proton-like and BKS models have been normalized to the data, in order to show the energy dependence of the cross-section.

to the control of the diffractive component of the cross-section, Monte Carlo models used to correct for the event selection cuts, the knowledge on absolute luminosity and shape of the luminosity spectrum. The errors are given in Table. 1, estimated using SIMDET [19] and extrapolations from HERA and LEP.

Fig. 3 shows present photon-photon cross-section data in comparison with recent phenomenological models [8]. Pseudo data points are added with a systematic error of 7%. The statistical errors are small since even for a day of running at a given energy only, $O(10^7)$ events are produced. Statistical samples of $10^4 - 10^5$ will be sufficient.

Table 1: List of systematic errors for the total cross-section measurement. The third column gives the source/reason

Type	Value	Comment
Selection cuts	3%	$\sim$HERA/frag. parameters
Diffraction	3-8%	$\rho\rho$ events
Detector smearing	3%	$\sim$HERA
Lumi/E_γ spectrum	3-4%	short runs ($\sim$ one day)
Bin correction	2%	$\sqrt{s_{\gamma\gamma}}$ spread

4 Precision necessary

In this section we show the numerical values corresponding to various predictions for the total $\gamma\gamma$ cross-section and indicate the precision needed to distinguish among these different models[21].

Table 2: Precision required for the measurement of $\gamma\gamma$ cross-sections to distinguish between the different 'proton' like models

$\sqrt{s_{\gamma\gamma}}(GeV)$	Aspen	BSW	DL	1σ
20	309 nb	330 nb	379 nb	7%
50	330 nb	368 nb	430 nb	11%
100	362 nb	401 nb	477 nb	10%
200	404 nb	441 nb	531 nb	9%
500	474 nb	515 nb	612 nb	8%
700	503 nb	543 nb	645 nb	8%

In Table 2 we show total $\gamma\gamma$ cross-sections for three models of the 'photon-is-like-the-proton' type. The last column shows the 1σ level precision needed to discriminate between Aspen[10] and BSW[11] models. The model labelled DL is obtained from Regge/Pomeron exchange with parameters from ref.[22] and factorization at the residues. The difference between DL and either

Aspen or BSW is bigger than between Aspen and BSW at each energy value. A similar table can be drawn for distinguishing between the two minijet formulations of Fig.1 and the BKKS model[13], for instance. The last column

Table 3: Precision required for the measurement of $\gamma\gamma$ cross-sections to distinguish between different formulations of the EMM and BKKS [13]

$\sqrt{s_{\gamma\gamma}}(GeV)$	EMM, Inel,GRS (p_{tmin}=1.5 GeV)	EMM, Tot,GRV (p_{tmin}=2 GeV)	BKKS GRV	1σ
20	399 nb	331 nb	408 nb	2 %
50	429 nb	374 nb	471 nb	9%
100	486 nb	472 nb	543 nb	11%
200	596 nb	676 nb	635 nb	6%
500	850 nb	1165 nb	792 nb	7 %
700	978 nb	1407 nb	860 nb	13 %

in Table 3 now gives the percentage difference between the two models which bear closest results, i.e. EMM with GRS densities and inelastic formulation on the one hand and BKKS, as well as EMM with GRV densities and total formulation on the other.

Hence, a detailed comparison of the predictions reveals that in order to distinguish between all the models the cross-sections need to be determined to a precision of better than 10% [8] at a future 0.5-1 TeV e^+e^-collider. This seems feasible from the simulation studies discussed above.

While the absolute cross-sections are measured with limited precision, the change of the cross-section with energy can be determined much more accurately. Fitting the data of the collider to the Regge inspired form s^ϵ in the high energy region, one can determine ϵ with a precision of $\Delta\epsilon = 0.02$. The models show a variation between $\epsilon = 0.08$ and $\epsilon = 0.26$.

5 σ_{tot} in the e^+e^- mode

It will be difficult to measure σ_{tot} with sufficient precision in the normal e^+e^- mode of the linear collider, however some information can be gained

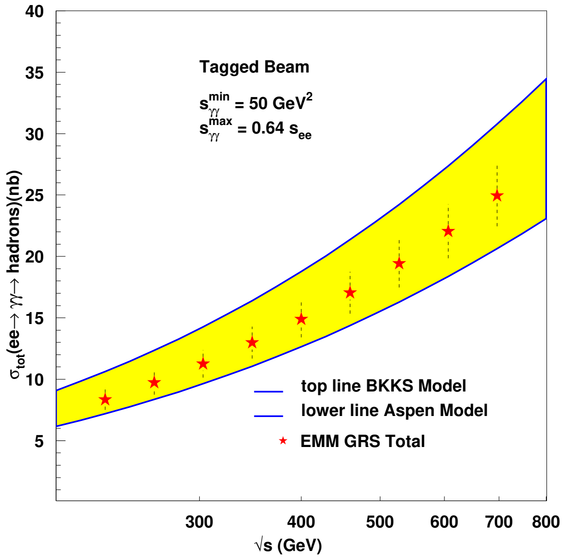

Figure 4: Cross-sections for hadron production due to $\gamma\gamma$ interactions in e^+e^- reactions.

from measuring the cross-section $\sigma(e^+e^- \to e^+e^- hadrons)$. This is calculated by convoluting the $\gamma\gamma$ *total* cross-section with the spectrum of these photons. This spectrum is given by the Weizsäcker Williams(WW) or effective photon approximation[15] which has been very successful in translating $\gamma\gamma$ cross-sections into e^+e^- ones. There have been many discussions of the improvements on the original WW approximation [23]. The discussion has also been extended to include the effects due to a reduction in the parton content of the photon due to virtuality of the photon [24]. The cross-section, including the effects due to (anti)tagging of the electron is given by

$$\sigma^{\rm had}_{e^+e^-} = \int_{zmin}^{1} dz_1 \int_{zmin/z_1}^{1} dz_2 \; f_{\gamma/e}(z_1) f_{\gamma/e}(z_2) \sigma(\gamma\gamma \to {\rm hadrons}). \qquad (1)$$

Here $zmin = s_{min}/s$ where $\sqrt{s}$ is the c.m. energy of the e^+e^- collider. The WW spectrum used is given by

$$f_{\gamma/e}(z) = \frac{\alpha_{\rm em}}{2\pi z}\left[(1+(1-z)^2)\ln\frac{P^2_{max}}{P^2_{min}} - 2(1-z)\right], \qquad (2)$$

where

$$P_{max}^2 = s/2 * (1 - \cos\theta_{tag})(1-z), P_{min}^2 = m_e^2 \frac{z^2}{(1-z)}.$$

Here, using θ_{tag} the maximal scattering angle for the outgoing electron, we have taken antitagging into account and have accounted for the suppression of the photonic parton densities due to virtuality following ref. [25].

To select $e^+e^- \to e^+e^- hadrons$ events, a minimum value $s_{\gamma\gamma}$ is required, selecting a region choosen such that it can be corrected for smearing and losses with sufficient precision. Also a maximum value is imposed, as for too large values of $s_{\gamma\gamma}$ the events resemble annihilation events, and cannot be easily separated. Additionally an anti tagging condition for the scattered electrons is imposed. SIMDET simulation studies lead to choose the region $50\ \mathrm{GeV}^2 < s_{\gamma\gamma} < 0.64 s_{ee}$, and the anti tagging cuts are $\theta_{\mathrm{tag}} = 0.025, E_{min}^e = 0.2 E_{\mathrm{beam}}$. With these cuts the total cross-section can be determined with a precision of 5-10%.

In Fig. 4, we show the cross-section as a function of $\sqrt{s}$ of the e^+e^- machine. The top curve corresponds to the prediction for $\sigma\gamma\gamma$ of the EMM model in the inelastic formulation and the lower curve corresponds to the prediction of the model [10] for the same. It is to be noted that the difference of about factor 2 (say) at $\sqrt{s} = 700$ GeV, is reduced to about $30-40\%$ after convolution with the bremsstrahlung spectrum. The 'data points' aregiven with a pessimistic error of 10%. Hence even in the worst of cases (no photon collider, large uncertainties in the e^+e^- $\sigma_{\gamma\gamma}^{tot}$ cross-section measurement) a linear collider will definitively contribute to a further understanding of the energy dependence of the total $\gamma\gamma$ cross-section.

6 Conclusions

Future linear e^+e^- colliders will be instrumental in the study of high energy photon collisions. We showed that new important information on the energy dependence can be extracted. The best option would be the photon collider mode, allowing for precise measurements at several $\sqrt{s_{\gamma\gamma}}$ energies. Accuracies of the order of 5-10% can be achieved, in a region where model predictions vary by a factor 2 or more. Even in the e^+e^- mode, there is sufficient sensitivity left in the total inclusive reaction $e^+e^- \to e^+e^- hadrons$, which does not require the reconstruction of $s_{\gamma\gamma}$, to distinguish between extreme model classes.

References

[1] D.Cline, F.Halzen and J. Luthe, Phys. Rev. Lett. **31** (1973) 491.

[2] M. Drees and R.M. Godbole, Phys. Rev. Lett. **67** (1991) 1189; P. Chen ,T. Barklow and M.E. Peskin, Phys. Rev. **D49** (1994) 3209, R.M. Godbole, hep-ph/9807379, Proceedings of the Workshop on *Quantum Aspects of Beam Physics, Jan. 5 1998 - Jan. 9 1998, Monterey, U.S.A.*, 404-416, Ed. P. Chen, World Scientific, 1999.

[3] For a review, see for example, M. Drees and R.M. Godbole, Journal of Phys. **G 21** (1995) 1559.

[4] L3 Collaboration, Paper 519 submitted to *ICHEP'98*, Vancouver, July 1998. M. Acciari et al., Phys. Lett. **B 408** (1997) 450; L3 Collaboration, A. Csilling, Nucl.Phys.Proc.Suppl. **B82** (2000) 239.

[5] L3 Collaboration, M. Acciari et al., hep-ex/0102025 (2001.)

[6] OPAL Collaboration. F. Waeckerle, *Multiparticle Dynamics 1997*, Nucl. Phys. Proc. Suppl. **B71**, (1999) 381, Eds. G. Capon, V. Khoze, G. Pancheri and A. Sansoni; Stefan Söldner-Rembold, hep-ex/9810011, To appear in the proceedings of the *ICHEP'98*, Vancouver, July 1998. G. Abbiendi et al.,Eur. Phys. J. **C14** (2000) 199.

[7] A. De Roeck, hep-ph/0101076 (2001).

[8] R. M. Godbole, G. Pancheri, hep-ph/0010104 (2000)

[9] G. Schuler and T. Sjöstrand, Zeit. Physik **C 68** (1995) 607; Phys. Lett. **B 376** (1996) 193.

[10] M.M. Block, E.M. Gregores, F. Halzen and G. Pancheri, Phys.Rev.**D58** (1998) 17503; M.M. Block, E.M. Gregores, F. Halzen and G. Pancheri, Phys.Rev. **D60** (1999) 54024.

[11] C. Bourelly, J. Soffer and T.T. Wu, Mod.Phys.Lett. **A15** (2000) 9.

[12] E. Gotsman, E. Levin, U. Maor, E. Naftali, Eur.Phys.J. C14 (2000) 511, hep-ph/0001080.

[13] B. Badelek, M. Krawczyk, J. Kwiecinski and A.M. Stasto. e-Print Archive: hep-ph/0001161.

[14] A. Corsetti, R.M. Godbole and G. Pancheri, Phys.Lett. **B435** (1998) 441.

[15] C.F. v. Weizsäcker, Z. Phys. **88**, 612 (1934); E.J. Williams, Phys. Rev. **45** 729.

[16] I.F. Ginzburg et al., Nucl. Inst. Meth. **A205** (1983) 47, **A219** (1984) 5; V.I. Telnov, Nucl. Inst. Meth. **A94** (1990) 72, `hep-ex/9908005`. R. Brinkmann et al., Nucl. Instrum. Meth. **A406** (1998) 13.

[17] V. Telnov, hep-ex/0101002 (2001).

[18] R. Engel and J. Ranft, Phys. Rev. **D54** (1996) 4244; R. Engel, Z. Phys. C66 (1995) 203.

[19] M. Pohl and J. Schreiber, DESY99-030 (1999).

[20] A. De Roeck, R. Engel and A. Rostovtsev, hep-ph/9710366.

[21] R. Godbole, A. Grau and G. Pancheri, *QCD and Multiparticle Production*, page 424. Proceedings of the XXIX International Symposium on Multiparticle Dynamics, Brown U., Aug. 2000. Eds. I. Sarcevic and C-I Tang. World Scientific 2000. e-print Archive: hep-ph/9912395.

[22] A. Donnachie and P.V. Landshoff, Phys. Lett. **B296** (1992) 227.

[23] For a recent discussion, see for example, S. Frixione, M.L. Mangano, P. Nason and G. Ridolfi, Phys. Lett. **B319**, 339 (1993).

[24] M. Drees and R.M. Godbole, Phys. Rev. **D50** (1994) 3124.

[25] M. Drees and R.M. Godbole, Zeit. Phys. **C59** (1993) 591.